A. M. Hassanein

Argonne National Laboratory,
Fusion Power Program.
Argonne, Ill. 60439

G. L. Kulcinski

University of Wisconsin,
Nuclear Engineering Department,
Madison, Wis. 53706

Simulation of Rapid Heating in Fusion Reactor First Walls Using the Green's Function Approach

The solution of the heat conduction probem in moving boundary conditions is very important in predicting accurate thermal behavior of materials when very high energy deposition is expected. Such high fluxes are encountered on first wall materials and other components in fusion reactors. A numerical method has been developed to solve this problem by the use of the Green's function. A comparison is made between this method and a finite difference one. The comparison in the finite difference method is made with and without the variation of the thermophysical properties with temperature. The agreement between Green's function and the finite difference method is found to be very good. The advantages and disadvantages of using the Green's function method and the importance of the variation of material thermal properties with temperature are discussed.

1 Introduction

Large energy deposition and intense heat fluxes are encountered on fusion reactor first wall components either due to x-ray and ion debris in Inertial Confinement Fusion (ICF) reactors or during a plasma dump in magnetic fusion reactors. Sizeable temperature excursions, resulting in melting and in some cases evaporation of the metallic components, have been observed [1, 2]. Although the analysis in this paper could be applied to any system where large energy deposition in short times is expected, the relation to fusion reactors is of particular importance to the design of the vacuum chamber. Recently a model has been developed by the authors [3] to accurately solve the heat conduction equation for this problem by finite difference methods. In this model, the surface temperature is determined by both the boundary conditions as well as by the kinetics of the evaporation process. The correct boundary condition entails partitioning of the incident energy flux into conduction, melting, evaporation, and radiation. Consequently, the heat conduction problem is one involving two moving boundaries, one being the melt-solid interface, and the other the surface receding as a result of evaporation. The kinetics of evaporation establish the connection between the surface temperature and the net atom flux leaving the surface, taking recondensation into account.

In this paper, the solution of this heat conduction problem in moving boundary conditions is presented by the use of the Green's function method. The Green's function method provides an easy and fast way of calculating the temperature rise within a reasonable range of accuracy. The finite difference approach consumes large computer time because of the limitations on both the maximum time step and zone thickness required for the stability of the solution. A comparison between the Green's function solution and the finite difference one developed in previous work [3] is also presented. This comparison with the finite differnece methods is made with and without the variation of the material thermal properties with temperature.

Although the results presented for carbon in this paper only consider one moving boundary at the surface because of vaporization (since carbon does not melt), the analysis is presented generally for the two moving boundaries to give a complete description of the possible transformations that can take place during rapid heating of wall materials.

2 Formulation of the Heat Conduction Problem

Consider the first wall or the area of deposition as a semi-infinite medium. This is reasonable in view of the short heat penetration depth during a plasma disruption in magnetic fusion rectors or target debris deposition in ICF reactors. Under a heat flux $F(t)$, the temperature distribution $T(x,t)$ must then satisfy the heat conduction equation

$$\rho c \frac{\partial T}{\partial t} - \nabla \cdot k \nabla T = \dot{q}(x, t) \tag{1}$$

where

ρ = density
c = specific heat
k = thermal conductivity
$\dot{q}(x, t)$ = volumetric energy deposition rate

All the thermophysical properties are functions of the local temperature. Initially the temperature is assumed to be constant throughout the material. The boundary conditions are that the back temperature, i.e., T_{back} = constant for large distances x and at any time t, and on the surface the heat flux is given by

$$F(t) = - k(T_v) \frac{\partial T}{\partial x} + \rho(T_v) L_v v(T_v) + \sigma \epsilon (T_v^4 - T_0^4) \tag{2}$$

where $T_v(t) = T(0, t)$, L_v is the heat of vaporization, and $v(T_v)$ is the velocity of the receding surface. This velocity is a function of the instantaneous surface temperature and other material parameters. Furthermore, the radiative heat transfer term contains the Stefan-Boltzmann constant σ; ϵ is the emissivity of first wall material; and T_0 is the surface temperature of the cold portion of the first wall inside the reactor cavity. For the radiative heat loss, it is assumed that parts of the first wall (mainly in magnetic fusion reactors) not struck by the plasma dump remain at the steady-state temperature T_0. Thus radiation heat flow is assumed from hot regions (T_v) where disruptions occur to the colder parts (T_0) of the unaffected areas. In ICF reactors, this term goes to zero since a microexplosion reaction is assumed to be symmetrical and the temperature will be the same everywhere.

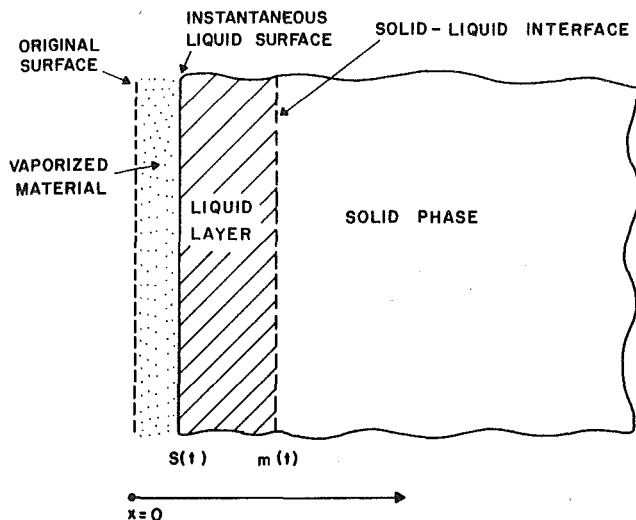The general heat-conduction equation with constant thermal properties can be written as

Fig. 1 Schematic representation of solid–liquid–vapor interfaces

$$\rho c \frac{\partial T}{\partial t} - k \nabla^2 T = \dot{q}(x, t) \tag{3}$$

where ρ, c, k are independent of temperature. For a semi-infinite medium, the Green's function is given by

$$G(x, t, x', t') = \frac{1}{2\sqrt{\pi \alpha(t - t')}} \{ e^{-\frac{(x-x')^2}{4\alpha(t-t')}} + e^{-\frac{(x+x')^2}{4\alpha(t-t')}} \} \tag{4}$$

where α is the thermal diffusivity. The general solution for the temperature rise due to any deposition function is given by [4]

$$T(x, t) = \int_{t'} \int_{x'} \frac{1}{\rho c} \dot{q}(x', t') G(x, t, x', t') dx' dt' \tag{5}$$

Once melting occurs, the condensed phase consists of two regions

(a) $s(t) \le x \le m(t)$ for the melt layer
(b) $m(t) \le x$ for the solid phase

where

$s(t)$ is the instantaneous distance of the melted surface.
$m(t)$ is the distance of the melted layer from the surface (as shown in Fig. 1).

The boundary conditions are now that at $x = m(t)$

$$T_s(m(t), t) = T_l(m(t), t) = T_m \tag{6a}$$

and

$$-K_l \frac{\partial T_l}{\partial x} \Big|_{m(t)} = -K_s \frac{\partial T_s}{\partial x} \Big|_{m(t)} + \rho_s L_f w(t) \tag{6b}$$

where T_m is the melting temperature; the subscripts s and l refer to solid and liquid regions, respectively; L_f is the latent heat of fusion; and

$$w(t) = \frac{dm}{dt} \tag{7}$$

is the velocity of the melt–solid interface.

If the heating is continued long enough and at a sufficiently high rate, significant vaporization may occur from the surface, assuming that the melting material stays in place. It is necessary to account for the receding surface at the interface between vapor and solid or liquid. This can be done by introducing a moving coordinate system

$$z(t) = x - s(t) \tag{8}$$

for which the surface always remains at $z = 0$. Transforming the heat conduction equation (1) or (3) to this moving frame gives

$$\rho c \left(\frac{\partial T}{\partial t} + \frac{\partial T}{\partial z} \cdot \frac{dz}{dt} \right) - \nabla \cdot k \nabla T = \dot{q}(z, t) \tag{9}$$

where

$$\frac{dz}{dt} = -\frac{ds(t)}{dt} = -v(t) \tag{10a}$$

$v(t)$ = velocity of the receding surface. This velocity is a highly nonlinear function of the surface temperature. Models to calculate surface velocity and evaporation are given in detail in (3). In these models, the surface velocity is given by

$$v(t) = 5.8 \times 10^{-2} \frac{x\sqrt{A} P_v(T_v)}{\rho(T_v)\sqrt{T_v}} [0.8 + 0.2 e^{-t/10\tau_c}] \text{cm/s} \tag{10b}$$

where

x = sticking probability (usually = 1)
A = atomic mass number
P_v = vapor pressure (Torr)
τ_c = vapor collision frequency (s^{-1}).

The kinetics of evaporation establish the connection between the surface temperatures and the net atom flux leaving the surface. Since the maximum temperature will be at the surface, no boiling phenomena is assumed to take place. Consequently, there is no specific temperature where a phase change from liquid to vapor phase can occur. Rather there is a continuous flow of vaporized atoms in which the rate of material removal depends only on the surface temperature, the corresponding vapor pressure, and the type of wall material.

Substituting equation (10a) into equation (9) gives

$$\rho c \frac{\partial T}{\partial t} - \rho c v(t) \frac{\partial T}{\partial z} - \nabla \cdot k \nabla T = \dot{q}(z, t) \tag{11}$$

The main difference in this equation is that it includes the convective term $v(t) \partial T / \partial z$. This term is important in the case of intensive evaporation if we are to obtain accurate calculations of the temperature. The surface boundary condition is then given by

$$F(t) = -k \frac{\partial T}{\partial z} \Big|_{z=0} + \rho L_v v(t) + \sigma \epsilon (T_v^4 - T_0^4) \tag{12}$$

where

$v(t)$ is again the velocity of the receding surface
$F(t)$ is the incident heat flux

Equation (11) can be written as

$$\rho c \frac{\partial T(z, t)}{\partial t} - k \nabla^2 T(z, t) = \dot{q}(z, t) + \rho c v(t) \frac{\partial T(z, t)}{\partial z} \tag{13}$$

The right-hand side of equation (13) consists of the volumetric energy deposition function and a convective term $\rho c v(t) \, \partial T / \partial z$, which could be treated as a part of the deposition function. Then equation (13) can written as

$$\rho c \frac{\partial T(z, t)}{\partial t} - k \nabla^2 T(z, t) = \dot{q}'(z, t) \tag{14}$$

where

$$\dot{q}'(z, t) = \dot{q}(z, t) + \rho c v(t) \frac{\partial T(z, t)}{\partial z} \tag{15}$$

The solution for the temperature rise due to the modified deposition function given by equation (15) and boundary condition in equation (12) is given by [5]

$$T(z, t) = \int_{t'} \int_{x'} \frac{1}{\rho c} \dot{q}'(z', t') G(z, t, z', t') dz' dt'$$

$$- \alpha \int_{t'} dt' G(z, t, 0, t') \frac{\partial T(0, t')}{\partial z} \qquad (16)$$

From equation (12) the gradient of the temperature can be represented by

$$k \frac{\partial T(0, t)}{\partial z} = \rho L_v v(t) + \sigma \epsilon (T_v^4 - T_0^4) - F(t) \qquad (17)$$

Substituting equation (17) and (15) into equation (16) yields

$$T(z, t) = \frac{1}{\rho c} \int_{t'} \int_{x'} (\dot{q}(z', t') + \rho c v(t') \nabla T(z', t'))$$

$$G(z, t, z', t') dz' dt' \qquad (18)$$

$$+ \frac{1}{\rho c} \int_{t'} G(z, t, 0, t')(F(t') - \rho L_v v(t') - \sigma \epsilon (T_v^4 - T_0^4)) dt'$$

where

$$\nabla T(z, t) = \frac{\partial T(z, t)}{\partial z}$$

$$T_v = T(0, t)$$

The difficulty in calculating the temperature rise from equation (18) is that both $v(t)$ and $\nabla T(z, t)$ are functions of the current temperatures, which are unknown. This is also true for the radiative heat transfer term in the second integral of equation (18). Although calculating the surface velocity, $v(t)$, requires only the knowledge of the surface temperature, the term $\nabla T(z, t)$ requires the current temperature distribution throughout the entire space.

A good approximation for the solution of equation (18) is to use the numerical techniques developed in [6]. In these techniques, space and time are divided into many divisions forming mesh points. The integrals over the time in equation (18) are replaced by a summation over the discrete values of time. The integration over the time is carried out from the initial time ($t = 0$) up to the time where the temperature is needed (i.e., T_n). The integration over space is carried out over the entire space. Each time integral term in equation (18) is replaced by two parts. The first part is a summation from the initial time and up to the time before the last (i.e., t_{n-1}). The second part is when the time approaches the time at which the temperature is needed (i.e., t_n). Then the solution for the temperature increase (at any point x_n and at time t_n) can be written as

$$T(x_n, t_n) = \sum_{t_i'=0}^{t_{n-1}} w_i \Delta t_i \int_0^\infty \frac{1}{\rho c} [\dot{q}(x', t_i') + \rho c v(t_i') \nabla T(x', t')]$$

$$G(x_n, t_n, x', t_i') dx'$$

$$+ w_n \Delta t_n \lim_{t_i' \to t_n} \int_0^\infty \frac{1}{\rho c} [\dot{q}(x', t_i') + \rho c v(t_i') \nabla T(x', t_i')]$$

$$G(x_n, t_n, x', t_i') dx'$$

$$+ \frac{1}{\rho c} \sum_{t_i'=0}^{t_{n-1}} \Delta t_i [F(t_i') - \rho L_v v(t_i') - \sigma \epsilon (T^4(0, t_i') - T_0^4)]$$

$$G(x_n, t_n, 0, t_i')$$

$$+ \frac{1}{\rho c} \Delta t_n [F(t_n) - \rho L_v v(t_n) - \sigma \epsilon (T^4(0, t_n)$$

$$- T_0^4)] \frac{1}{2\sqrt{\pi \alpha \Delta t_n}} e^{-(x_n^2/4\alpha \Delta t_n)} \qquad (19)$$

where

$T(x_n, t_n)$ is the temperature at any point x_n and time t_n.

w_i is a weighting factor depending on the method of integration.

Δt_i is the incremental time step.

In the second part of the first integral of equation (19), the Green's function possesses a singularity when $t_i' \to t_n$. To avoid this singularity, the last time step is made to be much smaller compared to any other time step, i.e.,

$$\Delta t_n << \Delta t_i \qquad (20)$$

where

$$t_{n-1} = t_n - \Delta t_n \qquad (21)$$

It can easily be shown that [6]

$$\lim_{\epsilon \to 0} \frac{1}{2\sqrt{\pi \alpha \epsilon}} e^{-\frac{(x-x')^2}{4\alpha\epsilon}} \to \delta(x-x') \qquad (22)$$

where $\delta(x-x')$ is the cronial δ-function. Using this result the last term of the first integral in equation (19) can now be written as

$$w_n \Delta t_n \int_0^\infty \frac{1}{\rho c} [\dot{q}(x', t_i') + \rho c v(t_i') \nabla T(x', t_i')] \lim_{t_i' \to t}$$

$$G(x_n, t_n, x', t_i') dx'$$

$$= w_n \Delta t_n \int_0^\infty \frac{1}{\rho c} [\dot{q}(x', t_i') + \rho c v(t_i') \nabla T(x', t_i')][\delta(x-x')$$

$$+ \delta(x+x')] dx'$$

It can also be shown that [4]

$$\left. \begin{array}{l} \int f(x', t) \delta(x-x') dx' = f(x, t) \\ \int f(x', t) \delta(x+x') dx' = f(-x, t) \end{array} \right\} \qquad (23)$$

Then substituting equation (22) in equation (19) and using the result from equation (23), the temperature rise in equation (19) reduces to

$$T(x_n, t_n) = \ldots + w_n \Delta t_n \frac{1}{\rho c} [\dot{q}(x_n, t_n) + \rho c v(t_n) \nabla T(x_n, t_n)]$$

$$+ \frac{1}{\rho c} \sum_{t_i'=0}^{t_{n-1}} \Delta t_i [F(t_i')$$

$$- \rho L_v v(t_i') - \sigma \epsilon (T^4(0, t_i') - T_0^4)] G(x_n, t_n, 0, t_i')$$

$$+ \frac{1}{\rho c} [F(t_n) - \rho L v(t_n) - \sigma \epsilon (T^4(0, t_n) - T_0^4)] \frac{1}{2\sqrt{\pi \alpha}} e^{-(x_n^2/4\alpha \Delta t_n)} \sqrt{\Delta t_n}$$

$$\qquad (24)$$

where

$$\int_0^\infty dx' \dot{q}(x', t_n) \delta(x_n - x') = \dot{q}(x_n, t_n)$$

and

$$\int_0^\infty dx' \nabla T(x', t_n) \delta(x_n - x') = \nabla T(x_n, t_n)$$

since

$$\dot{q}(-x_n, t_n) = 0$$

and

$$\nabla T(-x_n, t_n) = 0$$

Again the R.H.S. of equation (24) contains terms that are functions of the current unknown temperatures. These can be
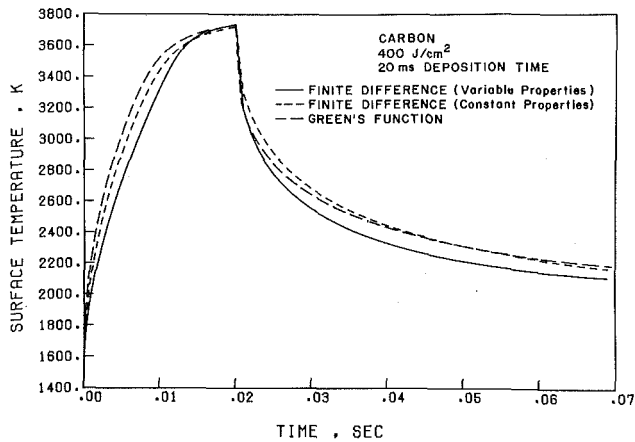
Fig. 2 Comparison of surface temperature rise for carbon for 400 J/cm^2 deposited in 20 ms by different methods

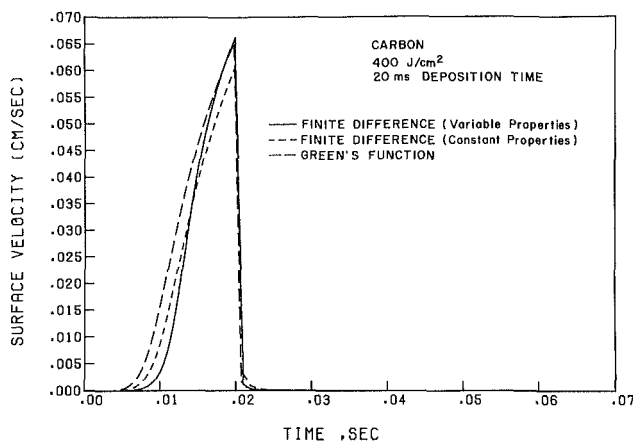Fig. 4 Evaporated material from carbon by different methods

Fig. 3 Carbon surface velocity for 400 J/cm^2 deposited in 20 ms by different methods

approximated by using the temperatures from the previous time step which are known. By choosing the increments between time steps small enough, the solution of equation (24) yields an accurate approximation to the integral equation (18). These choices always involve a compromise between accuracy and computer time. However, the required time step for these calculations is found to be much larger than the one required by the finite difference methods to solve the same problem.

The solution of equation (24) is implemented in the computer code A*THERMAL [7]. This equation can be used to determine the thermal response of fusion first walls both in inertial and in magnetic confinement reactors due to any kind of incident radiation, such as laser, x-rays, heat flux, or ions (light or heavy) for inertial confinement and plasma ions in magnetic confinement reactors.

3 Test Case

To test the accuracy of the solution for the moving boundary problem developed in this study, a comparison with the finite difference method is made. An example of the plasma disruption case [3] is considered where 400 J/cm^2 of plasma energy is deposited in a carbon first wall in 20 ms duration when the plasma suddenly and for unkown reasons becomes unstable. Carbon does not melt so only one moving boundary at the surface is considered in the solution of the heat conduction equation. The comparison is made between the finite difference with and without the variations of the
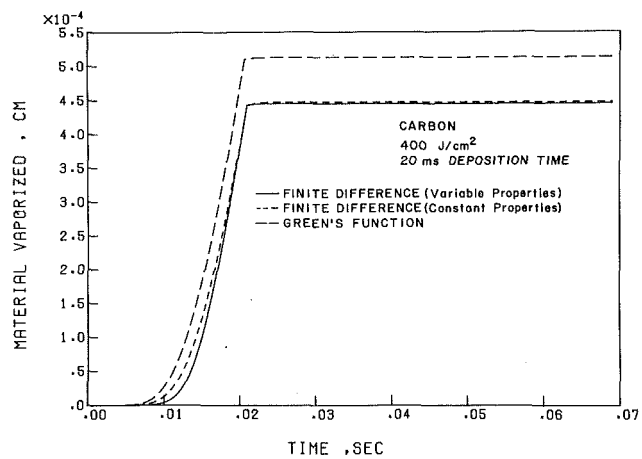
thermal properties with temperature. In the Green's function method, it is assumed that the thermal properties are constant and equal to those of the finite difference with constant properties. The thermophysical properties used in these calculations are given in [8]. Perturbation methods to account for the variation of thermal properties with temperature in the Green's function method are developed in [6]. A solution for the two moving boundaries problem where the material could change phase beside the surface moving boundary is also implemented in the computer code A*THERMAL.

4 Results and Discussion

The surface temperature as a function of the deposition time for the three methods, i.e., finite difference with variable properties, finite difference with constant properties, and the Green's function is shown in Fig. 2. The agreement between the Green's function and the finite difference with constant properties is very good as seen from Fig. 2. The little difference between the two methods, which is less than 3 percent, could be explained by the size of the time step chosen for each method. Although the Green's function method seems to require more calculations than the finite difference, its time step is much larger and its calculation is more straightforward than that for the finite difference approach. The effect of the variation of thermal properties on the surface temperature can also be seen from Fig. 2. The constant thermal properties chosen for Green's function and the finite difference were an average over a high temperature range. Because the lower the temperature, the higher the conductivity for carbon, the finite difference with variable properties has lower temperature than the other two methods either at earlier times in the pulse or at longer times after the end of the disruption.

The velocity of the receding surface, $v(t)$, as a function of time for the three methods of calculation is shown in Fig. 3. The lower surface velocity at earlier times for the finite difference with variable properties is due to the lower surface temperature because of higher thermal conductivity. The difference between the finite difference with constant properties and Green's function is also illustrated in Fig. 3. The agreement between the two methods is considered very good. The slightly higher velocity predicted by Green's function is due to the slightly higher surface temperature. Because of the highly nonlinear dependence of the surface velocity on the surface temperature, the difference between the surface velocity calculation by Green's function and by the finite difference methods is larger than the difference in calculating the surface temperature.

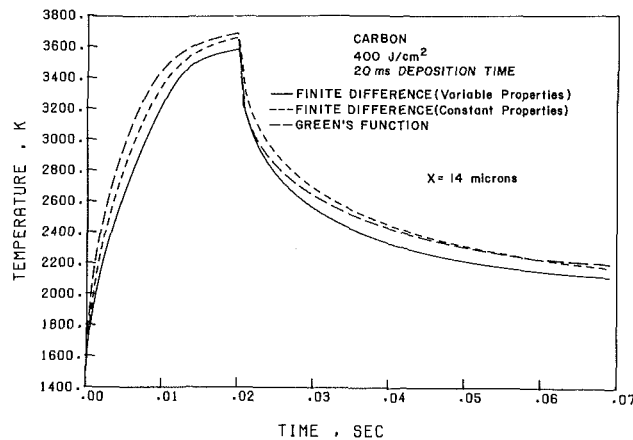The amount of the total material vaporized can be

Fig. 5 Comparison of temperature rise for carbon for 400 J/cm^2 deposited in 20 ms by different methods at x = 14 microns
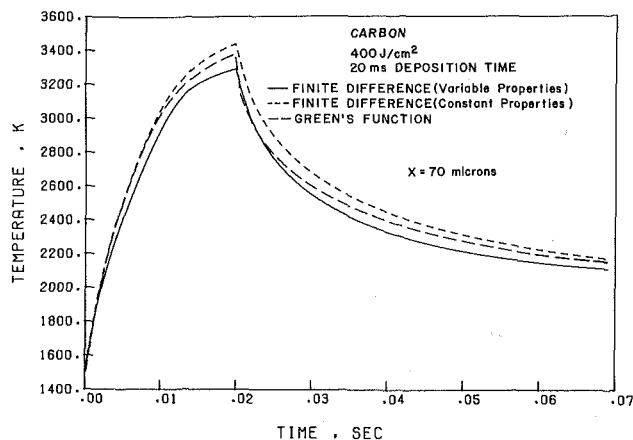

Fig. 6 Comparison of temperature rise for carbon for 400 J/cm^2 deposited in 20 ms by different methods at x = 70 microns

estimated by integrating the velocity of the receding surface over the pulse duration time. Figure 4 shows the amount of carbon varporized as calculated by the three different methods. The good agreement between both the finite difference methods, i.e., with and without the variation of thermal properties, is not because of the insignificance of the variation of the thermal properties with temperature, but rather because of the chosen value for the constant properties. This can be seen from Fig. 3, where although the velocity of the surface for the variable properties is lower at earlier times of the pulse, it becomes higher than the velocity for the constant properties near the end of the pulse. This incidentally has the effect of producing almost equal material vaporized from carbon for these two methods. On the other hand, Fig. 4 also shows about 10 percent higher total material vaporized by Green's function methods than the finite difference with constant properties. Although the surface temperature calculated using Green's function is only slightly higher than that calculated by the finite difference, and even lower after the end of the disruption time, the strong dependence of the evaporated material on the surface temperature and the integration of the surface velocity over all the pulse duration causes larger differences. After the end of the pulse the temperature drops very fast to where there is no significant

vaporization occurring. So the slightly lower surface temperature calculated by Green's function after the end of the pulse will not affect the total material evaporated.

The temperature distribution inside the bulk of the first wall material is also calculated using the three methods. Figures 5 and 6 show the temperature distribution of carbon at distance x = 14 and 70 microns from the surface. Because of the lower temperature inside the material, the difference (at x = 14 and 70 microns) between the finite difference with variable properties is larger than the difference between the other two methods. The larger the distance into the material, the lower the temperature and the larger the effect of the variation of the thermal properties. The agreement between Green's function and the finite difference with constant properties at larger distances into carbon is still very good, as can be seen from Figs. 5 and 6.

5 Conclusions

A method has been developed to solve the heat conduction problem with moving boundaries and other boundary conditions by the use of Green's function. The agreement of this solution with the method of the finite difference to solve the same problem is seen to be very good. The advantage of using the Green's function method is that it provides an easy and fast way of calculating the temperature rise in the material. This is because of no limitations on the time step or the mesh size used for the calculations. However, for more accurate results, the finite difference method is recommended, especially when evaporation is to be evaluated from these temperatures. The variation of the thermal properties with temperature can be very important in calculating accurate temperatures, especially in the case of very high energy depositions or if the material undergoes a change of phase. This is because of the larger differences between the solid- and liquid-phase properties. Because of the highly nonlinear dependence of the receding surface velocity on the surface temperature, a small change in calculating the surface temperature could result in large differences in the surface velocity, and consequently larger differences in calculating the total material removed from the surface by evaporation.

References

1 Cohen, S. A., et al., "Mechanisms Responsible for Topographical Changes in PLT Stainless Steel and Graphite Limitors," *Nuclear Fusion*, Vol. 21, 1981, pp. 233–249.

2 Sabado, M. M., et al., "*Doublet III Limiter Performance and Implications for Mechanical Design and Material Selection for Future Limiters,*" General Atomic Report GA-A15633, Oct. 1979.

3 Hassanein, A. M., Kulcinski, G. L., and Wolfer, W. G., "Vaporization and Melting of Materials in Fusion Devices," *J. Nucl. Mat.*, Vol. 103 & 104, 1981, pp. 321–326.

4 Carslaw, H. S., and Jaeger, J. C., *Conduction of Heat in Solids*, 2d ed., Oxford, 1959.

5 Ozisik, M. N., *Heat Conduction*, Wiley-Interscience, New York, 1980.

6 Hassanein, A. M., and Kulckinski, G. L., "Numerical Methods for Calculating the Temperature Increase in ICF First Walls," University of Wisconsin Fusion Engineering Program Report UWFDM-397, Nov. 1980.

7 Hassanein, A. M., "Thermal Effects and Erosion Rates Resulting from Intense Deposition of Energy in Fusion Reactor First Walls," University of Wisconsin Fusion Engineering Program Report UWFDM-465, Ph.D. thesis, Mar. 1982.

8 Rasor, N. S., and McClelland, J. D., "Thermal Properties of Graphite, Molybdenum and Tantalum, to Their Destruction Temperatures," *J. Phys. Chem. Solids*, Vol. 15, 1959, pp. 17–26.